ELSEVIER

Journal of Hazardous Materials 141 (2007) 115–122

Journal of Hazardous Materials

www.elsevier.com/locate/jhazmat

Adsorption of microcystin-*LR* by three types of activated carbon

Winn-Jung Huang [a,*], Bai-Ling Cheng [b,1], Yung-Ling Cheng [a]

[a] *Department of Environmental Engineering, Hung Kuang University, 34 Chung Chie Road, Sha-Lu, Taichung, Taiwan, ROC*
[b] *Environmental Toxins Laboratory, Hung Kuang University, 34 Chung Chie Road, Sha-Lu, Taichung, Taiwan, ROC*

Received 27 October 2005; received in revised form 26 June 2006; accepted 26 June 2006
Available online 4 July 2006

Abstract

The effect of carbon properties and water characteristics on the adsorption of m-*LR* by activated carbon was evaluated using kinetic and isotherm tests. The results showed that both physical and chemical effects simultaneously affect the adsorption process. The activated carbon with a high ratio of mesopore and macropore volume showed an increased m-*LR* adsorption capacity. The micropores in carbon offer only a nominal internal surface for adsorption. The adsorption capabilities of different activated carbon generally followed their pH_{zpc} values. Activated carbons with higher pH_{zpc} values exhibit a neutral or positive charge under typical pH conditions, promoting m-*LR* adsorption on the carbon surface. The competitive effects of natural organic matter (NOM) on activated carbon were evaluated and showed that caused a reduction in the capacity of carbon for m-*LR*. Furthermore, when pre-chlorination was preceded by adsorption, then the residual chlorine would react with activated carbon caused a decrease in sorption capacity of m-*LR*, while that chlorine at normal treatment plant dosages is not effective for degrading m-*LR*.

Keywords: Hepatotoxin; Microcystin-*LR*; Adsorption; Activated carbon; Natural organic matter; Mesopore

1. Introduction

The microcystins, hepatotoxic cyclic peptides, are one important group of cyanobacterial toxins. They are found in strains of *Microcystis*, *Oscillatoria*, *Anabaena* and *Nostoc* species and are involved in poisoning of animals and human health problems. Microcystins are extremely stable and resistant to chemical hydrolysis or oxidation at near neutral pH. In natural waters and in the dark, microcystins may persist for months or years [1]. Cyclic heptapeptide microcystins consist of five invariant amino acids and two variable amino acids. The invariant amino acids are in the *D*-configuration and the variable amino acids are in the *L*-configuration [2–5]. Different microcystins have different lipophilicities and polarities, which could affect their toxicity. Microcystin-*LR* (m-*LR*) was the first microcystin chemically identified; to date, most work has been conducted using this microcystin. It has been associated with most of the incidents of toxicity involving microcystins in most countries [6]. Recent epidemiological evidence results from studies of human populations that have shown symptoms of poisoning or injury (including hepatic illness, carcinogenesis and tumor growth promotion) attributed to the presence of microcystins in drinking water [7,8].

The health implication of drinking water treatment process performance in removing the microcystin toxins was detailed reviewed [9]. Conventional water treatment practices (pre-chlorination, coagulation/sedimentation, filtration, and post-chlorination) have been reported to be ineffective for removing mycrostins [10,11]. Water treatment studies conducted at the laboratory and pilot plant-scale have concluded that granular activated carbon (GAC) filtration is effective in removing the cyanobacterial toxins from drinking water [11–14]. Powdered activated carbon (PAC) was shown to remove the toxins but at doses higher than those are generally used at water treatment facilities [11,12,15]. Analysis of different brands of PAC at normal treatment plant dosages, evaluated in laboratory-purified water and in the presence of natural organic matter (NOM), showed that the PAC with the largest volume of mesopores (2–50 nm) adsorbed m-*LR* to the greatest extent [16].

The adsorption of relatively simple organic molecules from solvent or aqueous solution mainly depends on the adsorbent surface oxide concentration [17,18]. The solution pH also affects

* Corresponding author. Tel.: +886 4 26318652x4112; fax: +886 4 26525245.
E-mail addresses: huangwj@sunrise.hk.edu.tw (W.-J. Huang), octling@yahoo.com.tw (B.-L. Cheng).
[1] Tel.: +886 4 26318652x4118; fax: +886 4 26525245.

0304-3894/$ – see front matter © 2006 Elsevier B.V. All rights reserved.
doi:10.1016/j.jhazmat.2006.06.122

adsorption by activated carbon, due to adsorption surface chemical group preferential polarization. Jiang et al. [19] examined the effect of pH in the range 5–7 on humic acid adsorption by activated carbon and demonstrated that the adsorption affinity for humic acid decreased with increasing pH, interpreting their results in terms of the complex structure and solution properties. On the other hand, the drinking water treatment processes involve competitive adsorption between the adsorptive of interest and many other dissolved species classified as humic substances or dissolved organic matters. Such solution mixtures represent complex systems that are difficult to interpret unequivocally. Previous literature [16] discussed the competitive effects of NOM and pre-loading of organic matter on activated carbon to evaluate the effect of adsorption capacity and showed that both caused a reduction in the capacity of activated carbon for m-*LR*.

In this study, the adsorption of the m-*LR* onto the three types of activated carbon were studied and interpreted. Here the difference of adsorption kinetics and capacities are described and related to the characteristics of the carbons. The aim is to clarify the effects of carbon physical and chemical properties and as well as solution-phase chemistry as separate variables. The influence of water quality characteristics on the adsorption of m-*LR* by GAC was also evaluated in laboratory studies over a range of toxin concentrations similar to those typically observed in water.

2. Experimental

2.1. Materials

Microcystin-*LR* was purchased from Sigma–Aldrich (St. Louis, Missouri, USA). All reagents were either HPLC grade or analytical grade. Acetonitrile and trifluoroacetic acid were purchased from Merck. Methanol was obtained from J.T. Baker at HPLC grade. The m-*LR* stock solution was prepared at the concentration of 50 mg/L in methanol containing 0.1% trifluoroacetic acid. Deionized water was obtained by passing tap water through an Milli-Q system with the resistance >18.2 MΩ/cm and on-line TOC < 4 μg/L.

Three commercial types of GAC, namely, Norit (G1), Calgon (G2), and YUB (G3) with different origins were evaluated with kinetic and isotherm experiments. The main characteristics of selected GACs, such as raw material, mean particle size, total surface area, iodine number, hardness, abrasion, bulk density, and ash content are provided by the manufactures (Table 1). Acid and basic groups were determined by the acid–base titration procedure described by Siddiqui et al. [20]. The GACs for the kinetic and isotherm experiments were prepared by the following procedures: commercial GACs were pulverized and sieved to obtain 60 × 80 mesh particle sizes, resulting in an average particle diameter of 0.212 mm. After sieving, the carbons were washed with deionised water, and baked at 175 °C for 1 week to remove volatile impurities, and were then kept in the oven at 105 °C. Before use, the carbons were placed in desiccators and followed to cool to room temperature.

Table 1
Manufacturers' specifications of GACs used

Specifications	Norit[a]	F-400[b]	YUB[c]
Material	Coconut shell	Bituminous coal	Wood
Mean particle size (mm)	1.4	1.2	1.2
Total surface area (m^2/g)	950	950	1050
Iodine number (mg/g)	1020	1000	1000
Hardness (Ball-Pan, % min)	95	95	98
Abrasion number (%wt. min)	60	75	94
Bulk density (g/mL)	0.49–0.52	0.36–0.38	0.44–0.48
Ash content (%)	3	6.0	3

[a] Norit, Amersfoort, The Netherlands.
[b] Calgon Corporation, Pittsburgh, PA.
[c] China Carbon Corporation, Taipei, Taiwan, ROC.

As a further test of surface chemistry effects, we modified the surface chemistry of carbon G3 by cautious thermal reduction in an argon environment. The details of this treatment are described elsewhere [18]. The reduced samples, coded G3-T550 and G3-T950, signify thermal reduction at 550 and 950 °C for 1 h. Next, in order to investigate the influence of acid treatment in m-*LR* adsorption. Each types of carbon were immersed in 1 L of 6N HNO_3 at room temperature. After 24 h, the acid-treated carbons were thoroughly rinsed with distilled water and baked at 105 °C for 1 week. The acid-treated samples are coded G1-HA, G2-HA, and G3-HA, respectively.

2.2. Characterization of the carbons

The pore size distribution, BET surface area, macropore volume V_{macro}, mesopore volume V_{meso}, and micropore volume V_{micro}, of the samples were determined from N_2 adsorption and desorption isotherms measured at 77 K using an adsorption apparatus (ASAP 2010, Micromeritics Co., Georgia, USA). Pore size distribution and V_{meso} were evaluated by applying the Dollimore–Heal method [21] to the desorption isotherm, whereas the *t*-plot method [22] as used to estimate V_{micro}. The Dubinin–Astakhov equation [23] was applied to CO_2 adsorption data measured at 25 °C to determine V_{macro} of carbons.

The surface chemistry of carbons was determined by mass titration methods, in 0.1N NaCl, and acid–base depletion, from HCl–NaCl and NaOH–NaCl solutions were carried out on each sample to determine the acid–base properties of the carbons [24]. The oxygen content of the carbons was measured by hydrogen reduction techniques [25].

2.3. Water source

Treatment water, before chlorination, was used in this study. The water collected from the water treatment plant (Fen-San water treatment plant, FSWTP) for the major public water supply for Greater Kaohsiung area, the second largest metropolis in Taiwan with a population over 3 million. Owing to upstream discharge of farming, industrial, and domestic wastes, the reservoir has become eutrophic environment. As a result, growth of the cyanobacteria has been rapid, with an approach 250% increase during the past 10 years. Historically, dissolved organic car-

Table 2
Characteristics of water sources

Parameters	Range
pH	7.4–7.6
Alkalinity (mg/L as $CaCO_3$)	105–121
Turbidity (NTU)	<1
Conductivity (μs/cm)	547–936
Bromide (mg/L)	0.12–0.27
Chloride (mg/L)	17.3–23.6
Ammonia-nitrogen (mg/L)	<0.02
Dissolved organic carbon (mg/L)[a]	4.5–7.9
Hydrophobic fraction (mg/L)	1.4–3.7
Hydrophilic fraction (mg/L)	3.0–4.4
AOC (μg acetate-C/L)[b]	152–177
AOC_{P17} (μg acetate-C/L)	83–111
AOC_{NOX} (μg acetate-C/L)	52–68

[a] Dissolved organic carbon classified into hydrophobic and hydrophilic fractions.
[b] AOC classified into AOC_{P17} and AOC_{NOX}.

bon (DOC) in this source water has been as high as 8.5 mg/L, and its organic content was found to consist predominantly of hydrophilic organics. The other characteristics of the water sources studied during this research are summarised in Table 2.

2.4. Kinetic adsorption measurements

Kinetic adsorption of m-*LR* was run in a rotary tumbler using a rotation speed of 120 rpm. The appropriate carbon dose was introduced into 100 mL amber glass bottles. The carbon for the kinetic tests was soaked in Milli-Q water (buffered with 10 mM Na_2HPO_4/H_3PO_4, adjusted to pH 7.5 with HCl) overnight to promote wetting of the carbon surface and internal pore structure. Then injection of 500 μL of a 50 mg/L solution of m-*LR*, the m-*LR* concentration in bottle was 250 μg/L. The bottles were filled to exclude headspace with a m-*LR* solution and capped with Teflon septum caps. Then the bottles were put on a rotary tumbler with samples taken at predetermined intervals over 72 h. Samples were filtered through pre-washed 0.45 μm filters to remove the activated carbon and the residual m-*LR* concentrations were determined.

2.5. Adsorption isotherm measurements

The equilibrium adsorption isotherm for m-*LR* from a synthetic solution on activated carbon were determined at 25 ± 1 °C using a bottle-point method. Different amounts of carbon were weighed and added into 18 amber glass bottles, and 100 mL of m-*LR* solution (250 μg/L) was added to each of the bottles. In this part, we also used a non-porous carbon (inactivated coal) as a specific surface area standard for calibration purposes. The synthetic solutions were prepared with Milli-Q water, and were buffered with 10 mM Na_2HPO_4/H_3PO_4 at pH 7.5. The water containing NOM for competitive isotherms was collected just prior to the chlorination at the FSWTP. The water was filtered through a filter to remove debris then added into glass bottles. Injection of 500 μL of a 50 mg/L solution of m-*LR*, the m-*LR* concentration in bottle was 250 μg/L. The bottles were placed in a rotary tumbler, in a temperature controlled room, at 25 ± 1 °C and rotated at 120 rpm for 24 h.

2.6. Analytical methods

Analysis of microcystin-*LR* was performed by HPLC using a gradient mixer pump (LC-10AT, Shimadzu, Tokyo, Japan) equipped with a high-resolution diode array detector. For m-*LR* quantification a reference standard (Sigma, microcystin-*LR* from *Microcystis aeruginosa*, purity 95%) was used. The samples were concentrated with solvent–water evaporator systems (ASE 100, Dionex, CA) before analyzed by HPLC. The analysis was performed using a symmetry C18 (3.9 mm × 150 mm i.d.), 5 μm column. The injection volume was 100 μL and the flow rate of the mobile phase was 1.0 mL/min. The mobile phase was a mixture of Milli-Q water, ammonium acetate (10 mM; pH 7), methanol, and acetonitrile. All chromatograms were analyzed and integrated at 238 nm.

3. Results and discussion

3.1. Effect of GAC properties on adsorption kinetic of microcystin-LR

For m-*LR* adsorption it is important to recognize first that m-*LR* is a large molecule (MW = 994) and second that it is a complex aggregate of amino acids rendering hydrophobic character to its aqueous solution properties. Consequently, the correct selection of an activated carbon for m-*LR* removal from an aqueous solution, prior to any adsorption measurements, requires an appreciation of these properties combined with a detailed knowledge of the adsorbent's physical and surface chemical properties.

The typical N_2 adsorption–desorption isotherms for a sample of coconut shall (G1), bituminous coal (G2), and wood-based (G3) GACs are shown in Fig. 1a. The development of micropores and mesopores can be clearly confirmed by the shape of the isotherms. The porous properties of the GACs calculated from the isotherms are summarized in Table 3. The wood-based G3 carbon with highly V_{meso} value up to 0.76 cm^3/g is extremely higher than those of G1 and G2 carbons. Fig. 1b compares the pore size distributions of three types of GAC, where R_p and V_p are pore radius and pore volume, respectively. It was found that mesopores in the range of $2 < R_p < 12$ existed abundantly in the G3 carbon.

Table 3 also includes the chemical properties; bulk oxygen content and pH_{zpc} for each carbon. Clearly the wood-based carbon (G3) contains more oxygen than the coconut- and coal-based carbons. The heat-treated samples of G3 carbon show a decrease in oxygen content with increasing reduction temperature, reaching at 950 °C, an oxygen content similar to that of the hydrophobic carbons, in sample G1 and G2. Surface charge titration analyzes of these carbons show that the G3 carbon have the lower pH_{zpc} (4.1) than the other carbons. It can be concluded that the type and quantity of ionizable groups on these carbons are different. The change in surface charge with pH also indicates that the quantity and quality of surface ionizable groups is quite different for these carbons. The

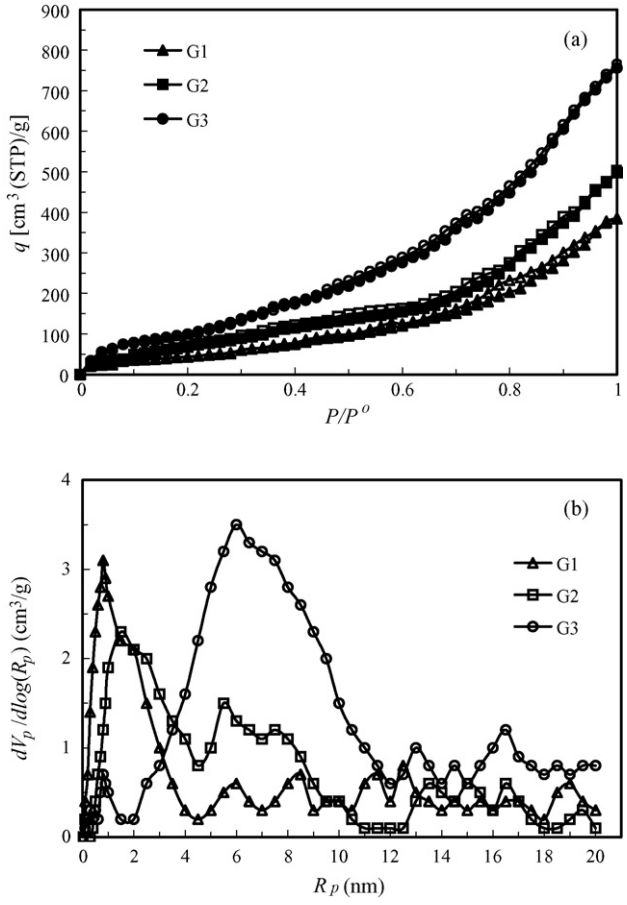

Fig. 1. (a) Nitrogen adsorption–desorption isotherms of GACs, and (b) pore size distributions of GACs.

change for the wood-based carbon is considerably stronger than that for the coal- and coconut-based carbons. The net surface charge for G2 carbon (-0.11 ± 0.24 mequiv./g) and G3 carbon (-0.68 ± 0.82 mequiv./g) are mainly negative, while G1 carbon (0.07 ± 0.25 mequiv./g) is mainly positive over the pH range 6–8.

Fig. 2 displays the batch kinetic removal curves, presented as the amounts adsorbed (q_e) versus contact time (t), achieved

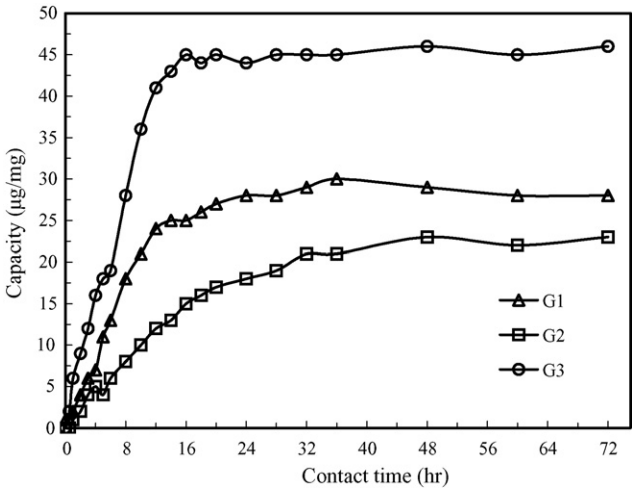

Fig. 2. Kinetic plots of m-*LR* adsorption by selected three GACs.

by the three carbons under consideration, for the m-*LR* single components. It is clear that 24 h are sufficient for attaining the equilibrium for all the adsorption systems. The amounts adsorbed by the three carbons are expressed in two estimates: capacity (mg/g or μmol/m^2) and the distribution coefficient, K_d (mL/g).

The kinetics of adsorption of m-*LR* on the three carbons is currently described on the basis of Eq. (1):

$$q_e = K_p t^{1/2} \quad (1)$$

where q_e is the instantaneous substrate concentrations on the adsorbent (mg/g), K_p the intraparticle diffusion rate constant, and t is the contact time (h). The evaluated adsorption rates for intraparticle diffusion, K_p, which are useful for comparative purposes, are given in Table 4. The plots covering the initial phase of adsorption (not shown) did not pass through the origin, indicating that pore diffusion may not be the only rate-controlling step in the removal of the adsorbates, especially for the early stages of adsorption. Considering K_p, the intraparticle diffusion rate constants listed in Table 4, the G3 carbon showed an obviously larger diffusion rate than the other two carbons. Due to its higher V_{meso} value, it is reasonable to assume that the mesopores of the

Table 3
Porous and surface properties of GACs

Carbon	V_{meso} (cm^3/g)	V_{micro} (cm^3/g)	Oxygen content (%)	pH_{zpc}	Acid (mequiv./g)	Basic (mequiv./g)	Hydroxyl groups (mequiv./g)
G1[a]	0.089	0.812	3.5	5.2	0.18	0.23	0.07
G1-HA[b]	0.072	0.816	–	–	0.20	0.16	0.03
G2	0.175	0.689	4.3	5.8	0.21	0.57	0.08
G2-HA	0.159	0.693	–	–	0.26	0.22	0.03
G3	0.760	0.242	11.5	4.1	0.23	0.71	0.26
G3-T550[c]	0.773	0.231	6.9	–	–	–	0.19
G3-T950[d]	0.781	0.194	4.2	–	–	–	0.10
G3-HA	0.736	0.277	–	–	0.44	0.33	0.11
G3-Cl[e]	0.755	0.256	7.6	–	0.32	0.56	0.33

[a] Virgin carbon.
[b] Acid washed with 6N HNO_3.
[c] Thermal reduction at 550 °C.
[d] Thermal reduction at 950 °C.
[e] Chlorinated with 1.5 mM NaOCl.

Table 4
Adsorption kinetics parameters for tested carbon samples

Carbon	K_p (mg/g h$^{0.5}$)	q_e (mg/g)	R^2
G1	0.118	14.5	0.951
G2	0.103	16.6	0.932
G3	0.431	73.7	0.984

carbon played an important role in the adsorption of large molecular adsorbates like m-*LR*. On the other hand, the extent of m-*LR* removal (adsorption capacity) was found to vary significantly from carbon to carbon, ranging from 37% to almost complete removal with an initial m-*LR* concentration of 15–250 μg/L. To gain a better understanding of the kinetic adsorption parameters showed in Table 4, the data were analyzed in terms of carbon properties, in particular, carbon porosity and pore size distribution. Since enhanced adsorption can be expected within pores of dimensions similar to the molecular dimension of the adsorptive [2], carbon pore size distributions were examined. Donati et al. [16] investigated the efficiency of m-*LR* adsorption by powder activated carbon and related its removal only to the mesoporosity of the activated carbons considered. In contrast with this and other previously published data examining pore volume influence on m-*LR* adsorption [14]. We show in Fig. 3, a correlation of the maximum average amount of m-*LR* adsorbed with the mesopore and macropore volumes for each GAC. Considering the good correlation suggested by the previous authors [2,16] and in our study, it is appropriate to suggest that any selection of an activated carbon for m-*LR* removal should consider both the mesopore volume and the macropore volume.

3.2. Effect of GAC properties on adsorption isotherm

The adsorption isotherms with carbons and m-*LR* solution in buffered Milli-Q water are shown in Fig. 4. The isotherms were

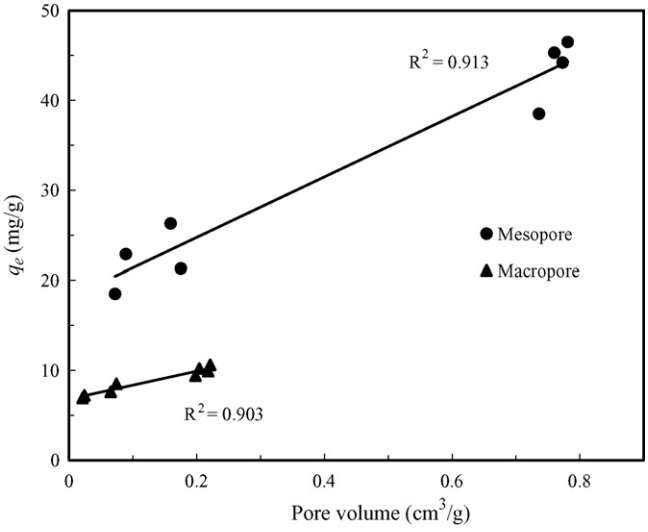

Fig. 3. Correlation of the q_e of m-*LR* adsorbed with the mesopore and macropore volumes.

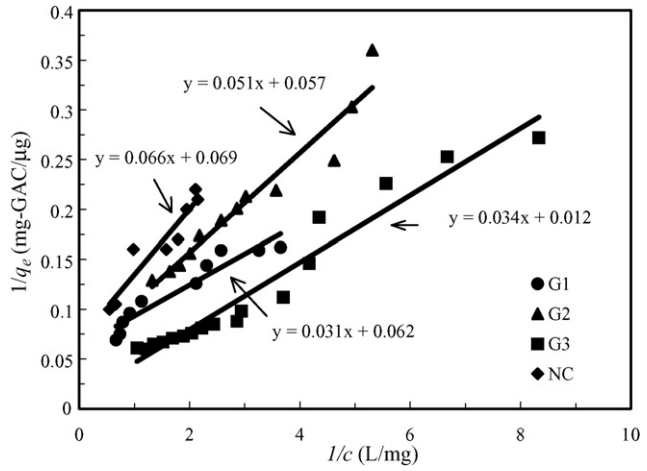

Fig. 4. Langmuir adsorption isotherms of m-*LR* on selected three GACs in buffered Milli-Q water.

interpreted in view of Langmuir isotherm model described by

$$\frac{1}{q_e} = \frac{1}{q_m} + \left(\frac{1}{q_m K_L}\right)\frac{1}{c} \quad (2)$$

where q_e and c are the concentration of m-*LR* in the activated carbon and solution, respectively, q_m the maximum sorption capacity, and K_L is a constant related to the adsorption energy (equilibrium constant of adsorption of m-*LR*). The calculated monolayer equivalent amount adsorbed and average maximum adsorbed by each carbon are summarized in Table 5. Generally, a good agreement exists between each set of data. In fact, there is a large difference in m-*LR* adsorption, illustrating the molecular sieve effect of activated carbons. Examination of Table 3 shows that, except for G3 carbon, all other carbons only have a small mesopore volume. The amount of m-*LR* adsorbed by the microporous coconut-shall and bituminous-coal based carbons are very similar to that for the non-porous carbon black (NC), even at high carbon dose of 500 mg/L that no significant increase in m-*LR* adsorption capacity was observed. Therefore, it can be suggested that the micropores in these carbons offer only a nominal internal surface for adsorption. Furthermore, the effect of surface chemistry on m-*LR* adsorption by activated carbon is probed by reducing the oxygen content of G3 carbon, without affecting its various pore volumes (see Table 3). In these measurements, m-*LR* is exposed to activated carbons with increasing hydrophobic character, but a constant volume space available for adsorption. In aqueous phase, surface oxygen groups were found to play an important role. In particular, it was found that an increased amount of carboxylic groups on the surface leads to increased water cluster formation. Also, this

Table 5
Isotherm parameters for tested carbon samples

Carbon	q_m (mg/g)	K_L (L/mg)	R^2
G1	16.1	2.00	0.912
G2	17.5	1.12	0.937
G3	83.3	0.35	0.948
NC	14.5	1.05	0.902

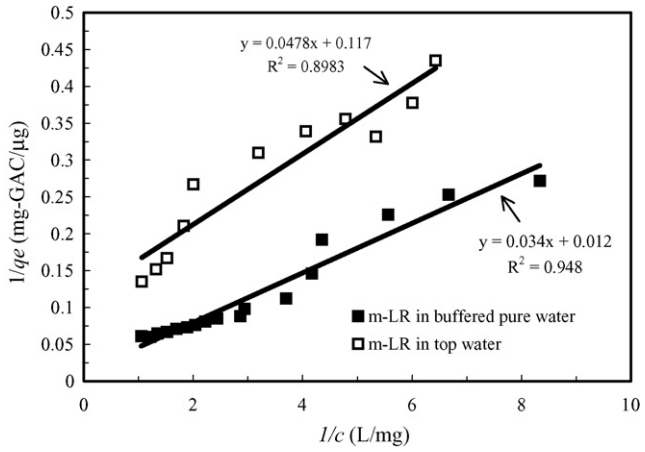

Fig. 5. Comparison of Langmuir adsorption isotherms of m-*LR* in buffered Milli-Q water within top water.

causes increased removal of π electrons from the basal planes [26], which would be resulted in weaker dispersion interactions with organic adsorbates. It is reasonable to presume that the influence of surface chemistry (oxygen content) applies at low adsorptive concentrations; hence the amount adsorbed in virgin carbon (oxygen content = 11.5%) is considerably lower than the two heat/hydrogen-treated carbons (oxygen content = 6.9 and 4.2%, respectively).

The other chemical characteristics obtained from analysis of the acid–base titration are presented first for virgin carbons and then for acid-washed carbons in Table 3. The indicated categories of surface chemical groups are classified according to their acid–base character. In a fixed pH 7.5, a well correlation was found between these groups and m-*LR* adsorption. The virgin carbon, which was more effective than acid-washed carbons for m-*LR* removal, was found to possess a much higher number of basic groups. The infrared spectra of these carbons indicate that the raw carbons contain more hydroxyl groups than the acid washed carbons. Generally, weak ionic interactions may participate in the adsorption of m-*LR* by the activated carbon surfaces in the form of an association of the positively charged arginine side chain of the toxin with the negatively charged carbon surface. From the discussion of carbon surface chemistry effects on m-*LR* adsorption, we suggest that both physical and chemical effects simultaneously affect the adsorption process.

3.3. Effect of water quality on m-LR adsorption

3.3.1. Effect of NOM

The competitive effect of NOM on m-*LR* adsorption was evaluated by conducting the adsorption isotherm experiments with water containing NOM, which was sampled from the Fen-San water treatment train just prior to entering the post-chlorination contact chamber. The isotherm with virgin G3 carbon and m-*LR* solution in buffered Milli-Q water, and the competitive isotherms with virgin G3 carbon and m-*LR* dissolved in drinking water are shown in Fig. 5. The maximum adsorbed capacity (q_m) of the carbon was observed to be much lower in the competitive isotherm compared with the Milli-Q water. Percentage m-*LR* removal decreased from 12% to 65%. The presence of NOM in the water has been shown to cause a reduction in the capacity of activated carbon for a number of target compounds [27,28] and for m-*LR* [16]. The NOM present in the Fen-San source water has been described as being high in hydrophilic organics (including hydrophilic -base, -acid, -neutral) [29]. The hydrophilic neutral generally represent the largest fraction of organic compounds of many polluted or eutrophic water. Many of identifiable, low molecular weight organics, and biodegradable organics was classified to the hydrophilic neutral fraction, and the percentage occupied in FSWTP's raw water is over 30%. Microcystin-*LR* has a molecular weight of 994, whereas the molecular weight distribution of DOC from FSWTP's waters is predominantly in the 500–10,000 ranges. On the other hand, the NOM present in algae–laden water has been described as being high in protein, amino acids, and polysccharides, and majority of algal cellular and extracellular substrates was found to be more polar than m-*LR* [30–32]. The NOM in the Fen-San water supply may have similar adsorption characteristics on activated carbon and thereby complete readily with m-*LR* for sorption sites. Moreover, the DOC of the water matrix used for the competitive isotherms was very high, 7.8 mg/L, compared to the m-*LR* (μg/L level). This large concentration difference between trace m-*LR* and bulk NOM was likely the main contributing factor for the decrease in capacity observed in the competitive isotherms.

3.3.2. Effect of pH

The adsorption of m-*LR* by three types of activated carbon was found to increase upon lowering pH from 8.0 to 3.0. The solid-phase concentration is reduced as pH increases beyond the pK_a because the anionic forms of m-*LR*, which are found at high pH, are not as well adsorbed. For most activated carbons investigated, the surface charge at high pH values is negative, which corresponds to the presence of negatively charged carboxylate and anhydride anionic surface functional groups on the activated carbon. In this study, the surface charge titration data indicate that the carbons move from a positively charged surface at pH 3.0 to a neutral charge at 5.2 (G1), 5.8 (G2), and 4.1 (G3), respectively, indicating an increase in negative charge. In the alkaline solution the m-*LR* also charged negatively. This means that there are no electrostatic forces between the carbon surface and the m-*LR* whereas the repulsion forces between the surface of carbon and m-*LR* occur. Moreover, the weak acidic functional groups of m-*LR* in low pH are undissociated (hydrophobic nature) and therefore are better adsorbed to the carbon surface than dissociated acidic functional groups at high pH. On the other hand, an electrostatic repulsion between neighboring negatively charged sites that cause stretching out of the molecules of m-*LR* is decreased with decreasing pH and as a result, m-*LR* molecules may become smaller in size due to the tendency to coil that reducing overall molecular dimensions [4]. Furthermore, the hydrogen bonds can also be formed between the coiled molecules and carbon surface charges at low pH, which leads to enhance the adsorption capacity. Therefore, it can be suggested that the change of molecular dimensions and the formation of hydrogen bonds are the main reasons for increasing

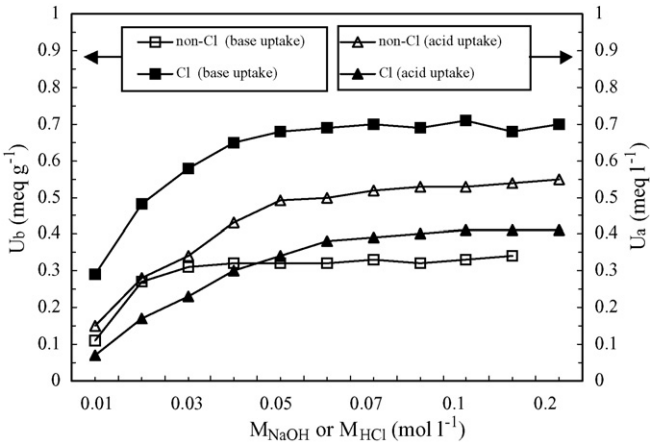

Fig. 6. Acid and base uptakes for virgin carbon (non-chlorinated carbon) and a chlorinated carbon (curves represent Langmuir fits calculated from the linear plots).

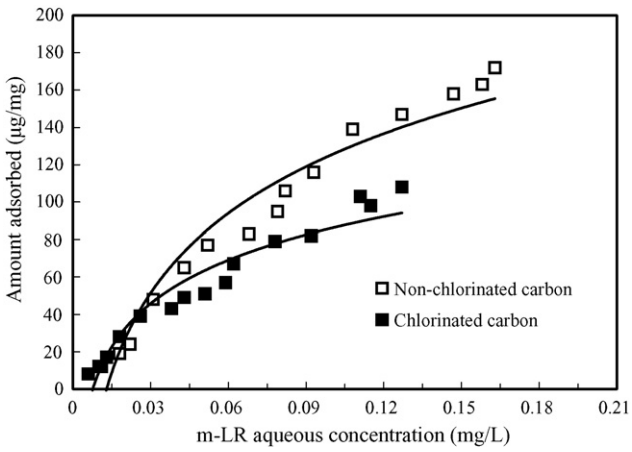

Fig. 7. Adsorption isotherms of m-*LR* for virgin carbon (non-chlorinated carbon) and chlorinated carbon.

adsorption with lowing pH between the m-*LR* and the carbon surface.

3.3.3. *Effect of chlorine*

The Langmuir monolayer capacities (q_e) for m-*LR* with and without chlorine in isotherm tests showed that the chlorine–carbon reactions reduced the m-*LR* adsorption capacity of the GAC. This implies that m-*LR* adsorption sites were preferentially occupied by either chlorine prior to surface reaction or by surface oxides. These results are consistent with those reported in the literature [33]. We suggest that both the interaction of chlorine with GAC surface and aqueous NOM have virtually influenced on the amount of m-*LR* adsorbed from pre-chlorination water.

In order to prove the reaction of chlorine and carbon surface and the relationship between chlorine fixation and other heteroatoms (such as oxygen and hydrogen) on the surface, the virgin carbon (carbon G3) has been treated with aqueous chlorine. Infrared spectroscopy analyzes of carbon surface show that the oxygen (O) in the chlorinated carbon exists as hydroxyl, carbonyl (quinone type), and lactone groups. Clearly the chlorinated carbon contains more oxygen than the virgin carbon (Table 3). It should be noted that the relationship between the total concentrations of surface acidic groups, measured by the amount of base uptake, with O is also different for the chlorinated carbons when compared to virgin carbons, reinforcing the observation that the chlorinated carbons are more acidic than the surface oxide concentration would indicate. A significant increase in base uptake from aqueous saline solution and decrease in acid uptake is observed when a chlorinated carbon is compared to the virgin carbon. Fig. 6 shows typical acid and base uptake for virgin carbon and a chlorinated carbon along with the respective Langmuir fits of the reaction isotherms. Base uptakes, $U_{b\infty}$, for the non-chlorinated and chlorinated carbons were 0.32 and 0.71 mequiv./g, respectively, while the acid uptakes, $U_{a\infty}$, for the same samples were 0.56 and 0.41 mequiv./g. Interestingly, the sum of the acidic and basic sites changes little, suggesting that the chlorination cause an inductive effect, making the oxygen sites more acidic but not actually creating or destroying the majority of these groups on the surface of the carbon.

Fig. 7 shows the m-*LR* adsorption isotherms on chlorinated and non-chlorinated wood-based carbon (G3) plotted on two different adsorption scales. The shape of the original m-*LR* isotherm seems to be retained and the equilibrium concentrations in chlorinated carbon are considerably lower than the non-chlorinated carbon indicating that the main differences are due to hydrophilic character, probably from the bonding of large Cl and O groups on the carbon surface. The effect of chlorination on m-*LR* adsorption by activated carbon is probed by using moderate chlorine doses (0.15 mM) for increasing the oxygen content of YUB carbon, and without affecting its various pore volume. In these measurements, m-*LR* is exposed to activated carbons with increasing hydrophilic character, but a practically constant volume space available for adsorption. These observations again indicate that surface chemistry has a significant effect on m-*LR* adsorption by the chlorinated carbon.

4. Conclusion

The effects of activated carbon properties and water characteristics on the capacity of m-*LR* adsorbed were evaluated and showed that both have virtually influence in the amount of m-*LR* adsorbed. Analysis of different properties GAC at used by treatment plant showed that carbons with the largest volume of mesopores and macropores adsorbed m-*LR* to the largest extent. On the other hand, due to the carbons containing larger mesopore and macropore size fractions, results in an enhanced intraparticle diffusion rate of m-*LR*. The functional group of carbon surface was also found to be an important factor in its ability to adsorb of m-*LR*. The carbons with the larger amounts of basic surface groups and higher pH_{zpc} showed the higher m-*LR* adsorption capacity suggesting that proton adsorption occurs on the available surface hydroxyl groups or phenolic groups at typical pH conditions.

The competitive effects of NOM were evaluated and showed that caused a reduction in the capacity of GAC for m-*LR*. The

large concentration differential between trace m-*LR* and bulk NOM was likely the main contributing factor for the decrease in capacity observed in the competitive isotherms. The adsorption of m-*LR* also affected by pH changes. An adjustment of the solution pH conditions, to low pH, results in an enhanced adsorption of m-*LR* due either to a decrease of the ionic interaction or to a changed molecular shape. The interaction of chlorine with activated carbon and NOM in raw water caused a decrease in m-*LR* adsorption. During the chlorination reactions, part of the NOM was converted to small MW and hydrophilic organics, leading to an increase compete with m-*LR* for sorption sites. On the other hand, activated carbon in chlorination water became more hydrophilic due to bond of large Cl and O groups on the carbon surface, thereby reducing the available adsorbent surface sites and, consequently, leading to a decrease in observed amount of m-*LR* adsorbed.

Acknowledgement

The authors thank the National Science Council, ROC, for financial support of this research under contract No. NSC 93-2211-E-241-005.

References

[1] L.R. Mur, O.M. Skulberg, H. Utkilen, Cyanobacteria in the environment, in: I. Chorus, J. Bartram (Eds.), Toxic Cyanobacteria in Water: A Guide to their Public Health Consequences, Monitoring and Management, World Health Organization, 1999.

[2] P. Pendleton, R. Schumann, S.H. Wong, Microcystin-*LR* adsorption by activated carbon, J. Colloid Interf. Sci. 240 (2001) 1–8.

[3] D.P. Botes, P.L. Wessels, H. Kruger, M.T.C. Runnegar, S. Santikorn, R.J. Smith, J.C.J. Barna, D.H. Williams, Structural studies on cyanoginosin-LR, -YR, -YA, and -YM; peptide toxins from *Microcystis aeruginosa*, J. Chem. Soc., Perkin Trans. I (1985) 2747–2752.

[4] T. Lanaras, C.M. Cook, J.E. Eriksson, J.A.O. Meriluoto, M. Hotokka, Computer modelling of the three-dimensional structures of the cyanobacterial hepatotoxins microcystin-*LR* and nodularin, Toxicon 29 (1991) 901–906.

[5] J.R. Bagu, F.D. Sonnicshsen, D.H. Williams, R.J. Anderson, B.D. Sykes, C.F.B. Holmes, Comparison of the solution structures of microcystin-*LR* and motuporin, Nat. Struct. Biol. 2 (1995) 114–116.

[6] J.K. Fawell, J. Hart, H.A. James, W. Parr, Blue-green algae and their toxins analysis, treatment and environmental control, Water Supply 11 (1993) 109–115.

[7] T. Kuiper-Goodman, I. Falconer, J. Fitzgerald, Human health aspects, in: I. Chorus, J. Bartram (Eds.), Toxic Cyanobacteria in Water: A Guide to their Public Health Consequences, Monitoring and Management, World Health Organization, 1999.

[8] A. Lankoff, W.W. Carmichael, K.A. Grasman, M. Yuan, The uptake kinetics and immunotoxic effects of microcystin-*LR* in human and chicken peripheral blood lymphocytes in vitro, Toxicology 204 (2004) 23–40.

[9] T.W. Lambert, C.F.B. Holmes, S.E. Hrudey, Microcystin class of toxins: health effects and safety of drinking water supplies, Environ. Rev. 2 (1994) 167–186.

[10] J.R.H. Hoffmann, Removal of *Microcystis* toxins in water purification processes, Water S.A. 2 (1976) 58–60.

[11] K. Himberg, A.M. Keijola, L. Hsvirta, H. Pyysalo, K. Sivonen, The effect of water treatment processes on the removal of hepatotoxins from *Microcystis* and *Oscillatoria* cyanobacteria: a laboratory study, Water Res. 29 (1989) 979–984.

[12] A.M. Keijola, K. Himberg, A.L. Esala, K. Sivonen, L. Hiisvirta, Removal of cyanobacterial toxins in water treatment processes: laboratory and pilot-scale experiments, Toxic Assess. 3 (1988) 643–656.

[13] I.R. Falconer, M. Runnegar, T. Buckley, V. Huyn, P. Bradshaw, Using activated carbon to remove toxicity from drinking water containing cyanobacterial blooms, J. Am. Water Works Assoc. 81 (1989) 102–105.

[14] T.W. Lambert, C.F.B. Holmes, S.E. Hrudey, Adsorption of microcystin-*LR* by activated carbon and removal in full scale water treatment, Water Res. 30 (1996) 1411–1422.

[15] I.R. Falconer, M. Runnegar, V. Huyn, Effectiveness of activated carbon in the removal of algae toxin from the potable water supplies: a pilot plant investigation, in: Proccedings of the 10th Federal Convention of the Australian Water and Wastewater Association, 1983.

[16] C. Donati, M. Drikas, R. Hayes, G. Newcombe, Microcystin-*LR* adsorption by powdered activated carbon, Water Res. 28 (1994) 1735–1742.

[17] K. Ogino, Studies in Surface Science and Catalysis, Elsevier, New York, 1992, pp. 491–498.

[18] R. Considine, R. Denoyel, P. Pendleton, R. Schumann, S.H. Wong, The influence of surface chemistry on activated carbon adsorption of 2-methylisoborneol from aqueous solution, Colloids Surf. A 179 (2001) 271–280.

[19] Z.P. Jiang, Z.H. Yang, J.X. Yang, W.P. Zhu, Z.S. Wang, in: J. Mallevialle, I.H. Suffet, U.S. Chen (Eds.), Influence and Removal of Organics in Drinking Water, Lewis, Boca Raton, 1992, pp. 79–88.

[20] M. Siddiqui, W. Zhai, G. Amy, C. Mysore, Bromate ion removal by activated carbon, Water Res. 30 (1996) 1651–1660.

[21] D. Dollimore, G.R. Heal, An improved method for the calculation of pore size distribution from adsorption data, J. Appl. Chem. 14 (1964) 109–114.

[22] B.C. Lippens, J.H. de Boer, Pore system *n* catalysts. V. The *t*-method, J. Catal. 4 (1965) 319–323.

[23] M.M. Dubinin, V.A. Astakhov, Description adsorption equilibria of vapors on zeolites over wide ranges of temperature and pressure, Adv. Chem. Ser. 102 (1971) 69–85.

[24] S.S. Barton, M.J.B. Evans, E. Halliop, J.A.F. MacDonald, Acidic and basic sites on the surface of porous carbon, Carbon 35 (1997) 1361–1366.

[25] M.C. Carlos, F.P.C. Agustin, M.H. Francisco Jr., C.M. Francisco, J.L.G. Fierro, Influence of carbon–oxygen surface complexes on the surface acidity of tungsten oxide catalysts supported on activated carbon, Carbon 41 (2003) 1157–1167.

[26] I.I. Salame, T.J. Bandose, Role of surface chemistry in adsorption of phenol on activated carbon, J. Colloid Interf. Sci. 264 (2003) 307–312.

[27] I.N. Najm, V.L. Snoeyink, Y. Richard, Effect of initial concentration of a SOC in natural water on its adsorption by activated carbon, J. Am. Water Works Assoc. 83 (1991) 57–63.

[28] S. Qi, V.L. Snoeyink, E.A. Beck, W.E. Koffskey, B.W. Lykins Jr., Using isotherms to predict GACs capacity for synthetic organics, J. Am. Water Works Assoc. 84 (1992) 113–120.

[29] W.J. Huang, H.H. Yeh, Reaction of chlorine with NOM adsorbed on powdered activated carbon, Water Res. 33 (1999) 65–72.

[30] C. Nalewajko, T.G. Dunstall, H. Shear, Kinetics of extracellular release in axenic algae and in mixed algal-bacterial cultures: significance in estimation of total (gross) phytoplankton excretion rates, J. Phycol. 12 (1976) 1–5.

[31] I.D. Campbell, R.A. Dwek, Biological Spectroscopy, Benjamin Cummings, Melano Park, California, 1984.

[32] E.W. Becker, Nutritional properties of microalgal: potential and constraints, in: A. Richmond (Ed.), CRC Handbook of Microalgae Mass Culture, CRC Press, Boca Raton, FL, 1986.

[33] M.J.B. Evans, E. Halliop, S. Liang, J.A.F. MacDonald, The effect of chlorination on surface properties of activated carbon, Carbon 36 (1998) 1677–1682.